https://dx.doi.org/10.1016/j.enconman.2023.117334

Load Allocation Methods for the Thermal and Electrical Chillers in Distributed Energy Systems for System Efficiency Improvement

Jiaqi Yuan[1,2#], Fu Xiao[2#], Wenjie Gang[1], Ying Zhang[3], Junxiao Shi[4], Zhenying Zhang[1], Xiuxia Hao[1]*

1. Department of Building Environment and Energy Engineering, School of Environmental Science and Engineering, Huazhong University of Science and Technology, Wuhan, China

2. Department of Building Environment and Energy Engineering, The Hong Kong Polytechnic University, Hong Kong

3. Institute of Artificial Intelligence, Huazhong University of Science and Technology, Wuhan, China

4. China Information Technology Design&Consulting Institute Co., Ltd.

 # The authors contribute equally to this paper.

** Corresponding author:*

Email: gangwenjie@hust.edu.cn

Address: School of Environmental Science and Engineering, Huazhong University of Science and Technology, Wuhan, China

Abstract:

Distributed energy systems fully utilize clean and renewable energy to satisfy the thermal and electrical loads of users. Absorption chillers are adopted to recover the waste heat from generators and are generally supplemented by electrical chillers or heat pumps to meet the insufficient thermal load. However, the load allocated to the absorption chillers can be affected by the heat pump/chiller owing to the chilled or hot water system distribution, leading to a lower energy utilization efficiency. In this study,

a new load allocation method is proposed in which the water flow rate (F-method) or supply temperature (T-method) of chilled/hot water systems is adjusted according to the cooling production capability of absorption chillers. The proposed method was verified using a distributed energy system serving a campus. The results showed that the cooling utilization ratio of the absorption chillers could be maintained close to 1, and the absorption chiller could follow the system waste heat well. Consequently, the primary energy efficiency and cost savings could be increased by 1.74% and 1.55%, respectively, and carbon emissions from the cooling systems could be reduced by 4.21%. This study can thus help improve the application and performance of distributed energy systems.

Keywords:

Distributed energy system; Load allocation; Absorption chiller; Electrical chiller; System efficiency; Carbon emissions reduction

Nomenclature

Abbreviations	
AC	Absorption chiller
AHU	Air handling unit
CCHP	Combined cooling, heating and power system
CE	Carbon emission (t)
COP	Coefficient of performance
CUR	Cooling utilization ratio
DES	Distributed energy system
ECR	Electric cooling ratio
F	Flow rate (kg/s)
Fac	Fraction
FCU	Fan coil unit
FEL	Following the electricity load
FHL	Following the hybrid load
FTL	Following the thermal load
GSHP	Ground source heat pump
HP	Heat pump
HVAC	Heating, ventilation and air conditioning
ICE	Internal combustion engine

num	Number
OC	Operation cost (CNY)
P	Power (kW)
PEE	Primary energy efficiency
PGU	Power generation unit
PLR	Part load ratio
PV	Photovoltaic
Q	Energy (kW)
T	Temperature (℃)
TES	Thermal energy storage
UA	U-factor times Area (W/k)
Symbols	
chw	Chilled water
ele	Electricity
exh	Exhaust gas
ext	External
int	Internal
jw	Jacket water
liq	Liquid
mec	Mechanical
noc	Nominal
ref	Reference
sha	Shaft

1 Introduction

Buildings contribute to approximately 47% of the total energy consumption [1], of which heating, ventilation and air conditioning (HVAC) systems use 50% [2]. A clean, efficient, and reliable energy supply for buildings is essential for energy conservation and reduction of national carbon emissions [3]. Distributed energy systems (DESs) can satisfy the energy demands of buildings with lower primary energy consumption and carbon emissions through a cascaded utilization of energy [4] and integration with local renewable energy [5]. DESs have been widely studied owing to their high efficiency, environmental friendliness[6], and supportive government policies[7]. However, as a DES contains many types of equipment, such as photovoltaics, heat pumps, and thermal energy storages, the system structure is increasingly complex. It is necessary to focus

on the operation strategy and control of the system to ensure its efficient and stable operation [8]. Many studies have proposed operation strategies to improve the adaptability of the system in different situations to improve its overall operating efficiency [9]. However, multiple chillers with different driving modes (thermal or electrical drives) are connected in parallel in DESs; therefore, appropriate water system control plays an important role in determining whether a DES can operate efficiently. Although several control methods are used for optimal load allocation on multiple chillers in HVAC systems, suitable water system control methods must be proposed based on the characteristics of DESs.

Combined cooling, heating, and power (CCHP) systems are typically the key configuration of DESs [10]. Internal combustion engines (ICEs) [11], gas turbines [12] and fuel cells [13] are used to provide electricity. The produced waste heat is recovered using absorption chillers or waste heat boilers to generate cooling or heating energy, respectively. Because the energy supply and load of the system cannot always match, boilers are added to provide the insufficient part of heat to drive the absorption chiller or satisfy the heating load of users [14]. The electrical boiler and three other technologies are integrated into the combined heat and power system to study their improvements in system flexibility and renewable energy accommodation. The results showed that using integrating electrical boilers is the most effective method to improve the accommodation of renewable energy [15]. Electrical chillers are used to satisfy the additional cooling load for users with high cooling loads [16]. The electricity consumption of the chillers can be provided by a power generation unit (PGU) or grid [17]. The primary energy efficiency of the system can be improved because of the high efficiency of the chiller. Particle swarm optimization algorithm is used for the optimal design of a DES with PGU, absorption chillers (AC), electrical chiller and thermal energy storage (TES). The results show that the DES is superior to the separate production system regarding energy, economic, and environmental performance [18]. Heat pumps (HPs) are alternatives to traditional boilers because they are more efficient

and can be used for both cooling and heating[19]. Ground source heat pump (GSHP) systems use soil as a cold and heat source; this can improve the operational efficiency of HPs owing to the low temperature variations in the soil throughout the year [20]. A CCHP system with GSHP is simulated and optimized to get the optimal capacity and the operation strategy considering the energy, environment, and economy criteria using Genetic Algorithm (GA). The case study shows that the primary energy saving ratio, carbon dioxide emission reduction ratio, and annual total cost saving ratio of the DES are 26.10%, 35.02%, and 15.13%, respectively, compared with the separated generation system [21]. GSHP can be combined with TES in the DES to improve system economic performance or reduce system capacity [22]. By using the GSHP to charge the TES at night and discharge the energy at peak hours, the total installed cooling capacity and heating capacity can be reduced by 15.8% and 37.5% [23]. The TES can also be integrated into the DES to utilize waste heat and improve the system performance. Under an appropriate control strategy, the primary energy efficiency can be increased by approximately 7% [24]. With the increasing penetration of renewable energy, multi-energy storage systems with batteries and thermal tanks are necessary for a supply–demand balance. Based on the cost-based site and capacity optimization of a multi-energy storage system, the integration of electrical and thermal storages can reduce the comprehensive costs by 8.1% and 5.3%, respectively [25]. However, while satisfying the increasing load and carbon reduction requirements, the structure of DESs has become increasingly complex. Consequently, to ensure efficient and stable operations of the system, good operation strategies are crucial.

The operation of a DES is considerably important to ensure that the system operates efficiently, particularly when renewable energy sources such as photovoltaics, solar thermal collectors, and wind turbines are integrated [9]. Following the electricity load (FEL) [26] and following the thermal load (FTL) are two classic and widely used strategies [27]. Based on these two strategies, following the hybrid load (FHL) strategy is proposed; it switches between the FEL and FTL strategies to avoid producing excess

energy[28]. A strategy for a DES that seasonally switches between FTL and FEL is proposed to improve the match between the load and the energy supply [29]. The electric cooling ratio (ECR) is considered in the operation strategies of DES with electrical chillers. The FEL-ECR and FTL-ECR strategies are proposed [30], where the cooling load is pre-divided into electric and absorption cooling parts to adjust the electricity output of the generators. As electrical chillers and TES provide flexibility for DESs, the power generator can operate based on the maximum efficiency [31] or daily average electricity load [32] to improve the system efficiency. To develop operation strategies under different load conditions, load matching maps of the DES are proposed, in which the operations of ICEs and HPs are determined according to the load points in different areas of the load matching map [33, 34]. An operation strategy based on the minimum distance is proposed to determine the operation of the PGU to reduce the excess energy and satisfy the demand [35]. A following system flexibility operational strategy that adjusting the state of charge of the storage devices actively is proposed to improve the flexibility of the CCHP system. Under the strategy, flexibility components can cover 93.75% of load scenarios and the dependence on the grid can be reduced by 98.04% and 99.61% [34]. Five dimensionless load matching parameters are used to describe the load matching map, and a hybrid load-following method is proposed based on the load matching map[36]. This method improved the system energy saving ratio by 10.1% and 0.7% on a typical summer and winter day, respectively. A following balanced heat-electrical load strategy is proposed based on the load matching map, which considers the electricity consumption of the HP to determine the operating point of the PGU[37]. Many strategies have been proposed to guide the system operation under different conditions; however, whether the system operates according to the applied strategy also depends on the control of the water system.

In heating, ventilation, and air conditioning (HVAC) systems, multiple chillers are connected as a group in parallel to obtain higher reserve capacity, operational flexibility, and efficiency [38]. Therefore, water system control is important for optimal load

allocation between chillers to minimize total energy use [39]. The average loading method is commonly used to operate multiple chillers. This is not the optimal solution, considering the different performance features and capacities of the chillers [40]. Therefore, many researchers have studied optimal control [41] and load distribution [42] for chilled water systems. Different optimization algorithms, such as the genetic algorithm (GA), particle swarm optimization (PSO), and differential evolution (DE), are used to determine the most suitable part load ratio of each chiller to obtain the best overall performance [39]. However, in DESs, unlike HVAC systems, chillers with different driving modes are connected in parallel. The absorption chillers driven by the waste heat from PGUs are expected to follow the PGUs without being affected by other chillers or loads. Therefore, different types of chillers have been proposed as a new requirement for the water system control of multiple chillers in DESs. Appropriate load allocation between the chillers is beneficial to improve the energy utilization efficiency of the system and reduce the power consumption of the electrical chillers, system operation costs, and carbon emissions.

The aforementioned review shows that several operation strategies for DESs have been proposed to enable complex systems to operate efficiently. However, the present strategies mainly focus on the operation of the PGU and assume that the absorption chillers can follow the PGU well. The available waste heat from the PGU determines only the maximum energy production of the AC. The operation of absorption chillers (ACs) is not only related to waste heat, but is also affected by chilled water systems. Therefore, without appropriate water system control of the load allocation between ACs and HPs, the ACs cannot guarantee that they follow the PGU well and fully utilize the available waste heat under changing electricity and cooling loads. The system operation deviation problem can lead to lower system primary energy efficiency and economic performance; therefore, appropriate load allocation control methods between thermal- and electrical-driven chillers/HPs are essential.

Therefore, to solve the aforementioned system operation deviation problem, this study primarily performed the following:

(1) A load allocation control method between thermal- and electrical-driven chillers/HPs in DESs was proposed to improve system operation efficiency.

(2) The proposed load allocation method was assessed under linearly changing user electricity and cooling loads to prove its effectiveness compared with that of the traditional constant flow method.

(3) The proposed load allocation method was studied in a DES on typical days and compared with different allocation methods to further demonstrate its improvements in terms of system energy efficiency, economy, and environmental performance.

(4) A load adaptability study was conducted to study the performance of the proposed methods considering different electricity and cooling loads, with the aim of identifying better application scenarios and quantifying energy-saving potentials.

The subsequent organization of the paper is as follows. In Section 2, the system operation deviation problem and the proposed load allocation method are described. Also, the modeling and evaluation criteria of the distributed energy system are introduced. In Section 3, based on the case study, the performance of the proposed methods is analyzed and discussed. Finally, conclusions are summarized in Section 4.

2 Methodology

This section first describes the system operation deviation problems in the operation of the distributed energy system. The proposed load allocation method that adjusts the flow rate (F-method) or the temperature (T-method) of the HPs is introduced for better load allocation between absorption chillers and heat pumps, ensuring the systems follow the PGU well and improve the system efficiency. Then, the configuration and the modeling of the distributed energy system are introduced. Finally, the evaluation

criteria used in the performance analysis are introduced.

2.1 System operation deviation problems in distributed energy systems

In a DES with ACs and HPs, the ACs typically operate based on the available waste heat from the PGU to produce cooling energy, and an insufficient load is provided by the HPs. When ACs operate in parallel with electrical chillers or HPs (which is a common situation in practice), the cooling or heating supplied by the ACs or HPs is also affected by the chilled or hot water distribution, respectively, on the user side. Under a certain water flow distribution and chilled water set point, the load allocation between the ACs and the HPs is settled [43]. This problem causes the system operation to deviate from the operation strategy, leading to a lower system primary energy efficiency and economic performance.

To illustrate this problem, the system structure is shown in Fig. 1 (Images of the absorption chiller and heat pump are from [44] and [45]), where the ACs and HPs are typically connected in parallel. The chilled water from the ACs and HPs is collected and sent to the end user via a communal pipe. After exchanging heat via fan coils or air handling units at the end-user, the return water is distributed to each unit. The AC is expected to operate following the waste heat from the PGU, as shown in Eq. (1) [34]. However, the actual operating state of an AC is related to the load and water system control parameters. The insufficient part of the cooling is supplied by the HPs according to the energy balance, as shown in Eq. (2) [23]. Because the ACs and HPs are connected in parallel, their cooling production exhibits a certain relationship. As shown in Eq. (3) [43], return water temperatures of the ACs and HPs are the same, and the cooling allocated to the HPs and ACs depends on the water flow rate and chilled water set points. Where, $Q_{\text{heat.ICE}}$ is the available waste energy from PGUs. COP_{AC} is the coefficient of performance of ACs. Q_{load} is the total cooling load supplied by the AC ($Q_{\text{chw,AC}}$) and the heat pumps ($Q_{\text{chw,HP}}$). num_{AC} and num_{HP} are the operating number of the AC and HP. $F_{\text{chw,AC}}$ and $F_{\text{chw,HP}}$ are the chilled water flow rate of the AC and HP. $T^{\text{out}}_{\text{chw,AC}}$

and $T_{\mathrm{chw,HP}}^{\mathrm{out}}$ are the supply water temperature of the AC and HP. T_{return} is the return water temperature. If the flow rate and supply water temperature of the chillers are determined, the ratio of $Q_{\mathrm{chw,AC}}$ to $Q_{\mathrm{chw,HP}}$ is constant, and the values of $Q_{\mathrm{chw,AC}}$ and $Q_{\mathrm{chw,HP}}$ can be determined under a specific load by combining Eqs. (2) and (3). The cooling produced by the AC cannot be guaranteed to be identical to that in Eq. (1). In other words, the AC may not follow the waste heat well, and the waste heat may not be fully used under the influence of the load side without appropriate load allocation control methods for the load allocation between chillers. This would lead to a lower primary energy utilization ratio, so it is necessary to adjust the flow rate or temperature at the load side so that the absorption unit can be allocated with a suitable cooling load to make full use of the waste heat.

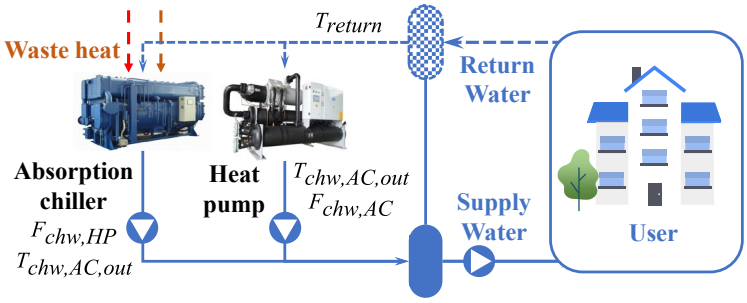

Fig. 1 Water system in the DES

$$Q_{\mathrm{chw,AC}}=Q_{\mathrm{heat.ICE}}\times\mathrm{COP}_{\mathrm{AC}} \tag{1}$$

$$Q_{\mathrm{load}}=Q_{\mathrm{chw,AC}}+Q_{\mathrm{chw,HP}} \tag{2}$$

$$Q_{\mathrm{chw,AC}}=\frac{\mathrm{num}_{\mathrm{AC}}\times F_{\mathrm{chw,AC}}\times(T_{\mathrm{return}}-T_{\mathrm{chw,AC}}^{\mathrm{out}})}{\mathrm{num}_{\mathrm{HP}}\times F_{\mathrm{chw,HP}}\times(T_{\mathrm{return}}-T_{\mathrm{chw,HP}}^{\mathrm{out}})}\times Q_{\mathrm{chw,HP}} \tag{3}$$

2.2 The proposed load allocation method

To avoid the system operation deviation problem, an improved load allocation method is proposed by adjusting the flow rate or supply temperature of HPs, as shown in Fig. 2. In the first stage, the system operation strategy determines the operating number of each unit in the system. The operation of ICEs is based on the electricity load. The number of working ACs is determined based on the open number of the ICE and cooling

load. Finally, the cooling supply and cooling load are compared to determine the operating status of the HP.

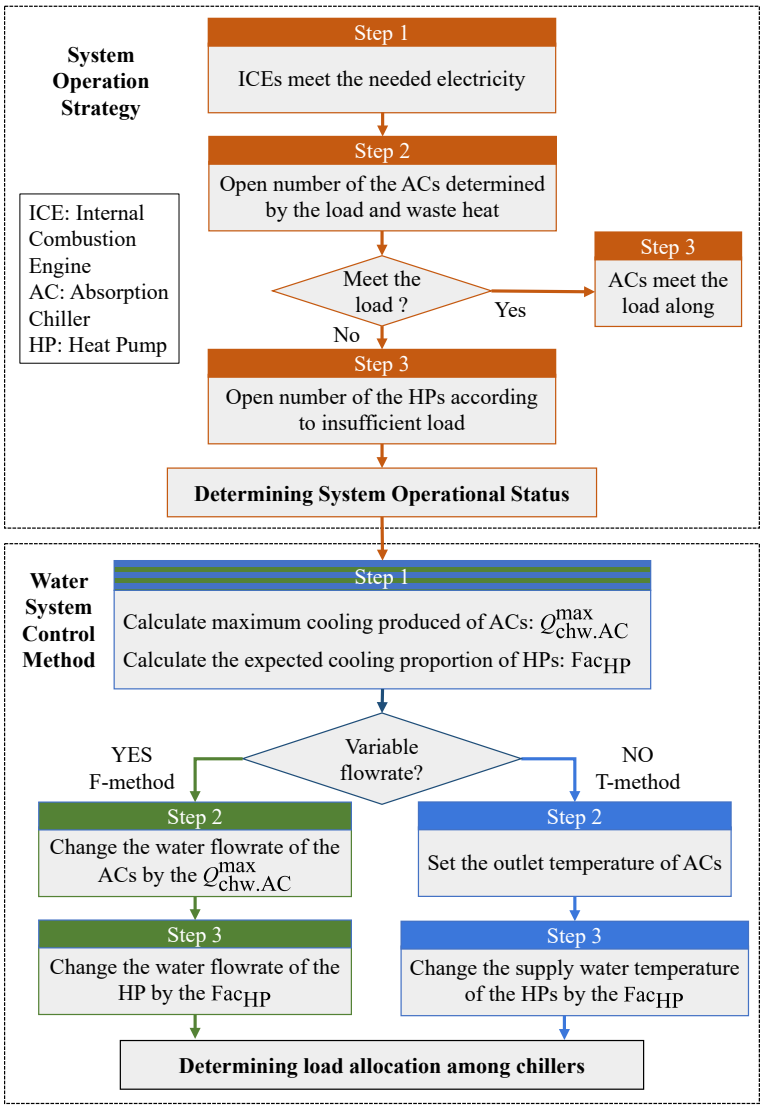

Fig. 2 The proposed load allocation method based on flow rate and temperature control

If the AC and HP run simultaneously to satisfy the cooling load, the load distribution among the two types of chillers must be considered based on the water system controls as per the analyses provided in Section 2.1. Control methods for the chilled water system are required to allocate a suitable cooling load to the absorption chillers to fully utilize the waste heat. Based on the aforementioned system operation strategy, the proposed load allocation method is used to control the water system in the second stage

to ensure that the system follows the ICEs well according to the operation strategy that includes the following steps:

(1) First, the maximum cooling supply of the ACs, $Q_{\text{chw.AC}}^{\max}$, is calculated under the current conditions. As shown in Eq. (4) [34], it depends on the current waste heat from the exhaust gas, waste heat from the jacket water, and COP of the ACs.

$$Q_{\text{chw.AC}}^{\max}=(Q_{\text{exh}}+Q_{\text{jw}})\times\text{COP}_{\text{AC}} \tag{4}$$

(2) Then, the expected cooling supply proportion of the HPs, Fac_{HP}, is calculated based on the energy balance, as shown in Eq. (5) [23], that is calculated based on user load Q_{load}, the maximum cooling supply of the ACs, and number of HPs.

$$\text{Fac}_{\text{HP}}=\frac{Q_{\text{load}}-Q_{\text{chw.AC}}^{\max}\times\text{num}_{\text{AC}}}{\text{num}_{\text{HP}}}/Q_{\text{load}} \tag{5}$$

(3) The load allocation control is implemented for both variable flow and constant flow systems.

✧ For the variable flow systems, the water flow rate between the ACs and the HPs is varied (F-method). The water flow rate to the ACs, $F_{\text{chw,AC}}$, is calculated according to the maximum cooling supply based on the load distribution law of the water system, as shown in Eq. (6) [43]. Where, the rated flow rate of the AC $F_{\text{chw.AC}}^{\text{rated}}$ is multiplied by the ratio of the maximum cooling capacity under the current waste heat $Q_{\text{chw.AC}}^{max}$ to the rated cooling capacity $Q_{\text{chw.AC}}^{\text{rated}}$. The calculated flow rate needs to be larger than the minimum allowable flow rate $F_{\text{chw.AC}}^{\min}$. The flow rate to the HPs is then determined according to the expected cooling supply proportion of the HPs, based on the load distribution characteristics, as shown in Eq. (7) [43], which is calculated by the water flow rate $F_{\text{chw,AC}}$ and open number num_{AC} of the ACs, the expected cooling proportion Fac_{HP} and the open number num_{HP} of the HPs. In addition, the flow rate should be higher than the minimum allowable flow rate of the HP, $F_{\text{chw.HP}}^{\min}$.

$$F_{\mathrm{chw,AC}}=\mathrm{MAX}\left(F_{\mathrm{chw.AC}}^{\mathrm{rated}}\times\frac{Q_{\mathrm{chw.AC}}^{\max}}{Q_{\mathrm{chw.AC}}^{\mathrm{rated}}},F_{\mathrm{chw.AC}}^{\min}\right) \tag{6}$$

$$F_{\mathrm{chw,HP}}=\mathrm{MAX}\left(\mathrm{Fac_{HP}}\times\frac{F_{\mathrm{chw,AC}}\times\mathrm{num_{AC}}}{1-\mathrm{Fac_{HP}}\times\mathrm{num_{HP}}},F_{\mathrm{chw.HP}}^{\min}\right) \tag{7}$$

✧ For constant primary water systems, the supply temperature of the HPs, $T_{\mathrm{chw,HP}}^{\mathrm{out}}$, is varied (T-method) according to the expected cooling supply proportion. Based on the characteristics of the water system load distribution, as shown in Eq. (8) [43], the supply temperature depends on return water temperature T_{return}, the expected cooling proportion, open number, and outlet temperature of the ACs $T_{\mathrm{chw,AC}}^{\mathrm{out}}$.

$$T_{\mathrm{chw,HP}}^{\mathrm{out}}=T_{\mathrm{return}}-\mathrm{Fac_{HP}}\times\frac{F_{\mathrm{chw,AC}}\times\mathrm{num_{AC}}\times\left(T_{\mathrm{return}}-T_{\mathrm{chw,AC}}^{\mathrm{out}}\right)}{\left(1-\mathrm{Fac_{HP}}\times\mathrm{num_{HP}}\right)\times F_{\mathrm{chw,HP}}} \tag{8}$$

2.3 System configuration and modeling

The DES configuration is shown in Fig. 3. On the energy supply side, different types of devices are coupled in a DES to provide electricity and cooling and heating energy to users. ICEs and photovoltaics are installed to satisfy the electrical load. An insufficient electricity load is obtained from the grid. The waste heat of the ICE is transferred to the jacket water and exhaust smoke. They are then be delivered to an AC to produce chilled water. The generator operates according to the electricity demand; therefore, the cooling energy generated by the ACs may be higher or lower than the cooling demand. Therefore, thermal energy storage systems are typically used to store surplus energy, and HPs are used to meet insufficient cooling or heating demands. All the cooling or heating energy must be sent to the user by the water system and driven by pumps. The chilled water system is a primary constant and secondary variable flow rate system. Primary pumps provide the pressure to circulate water through the chillers and other auxiliary equipment. Secondary pumps are used to provide water to the users. The primary flow rate is the sum of the flow rates of the operating ACs and HPs. The secondary flow rate is determined from the total flow rate of the terminal units on the demand side. A bypass pipe is used to balance the water flow rates between the primary and secondary sides. On the demand side, air handling units (AHUs) and fan coil units

(FCUs) are used to supply air to rooms to create a comfortable thermal environment for occupants. The AHUs treat fresh air to the isoenthalpy point of the indoor air. The indoor heat gain is eliminated using chilled water coils. PID controllers are used to adjust the flow rate of each unit.

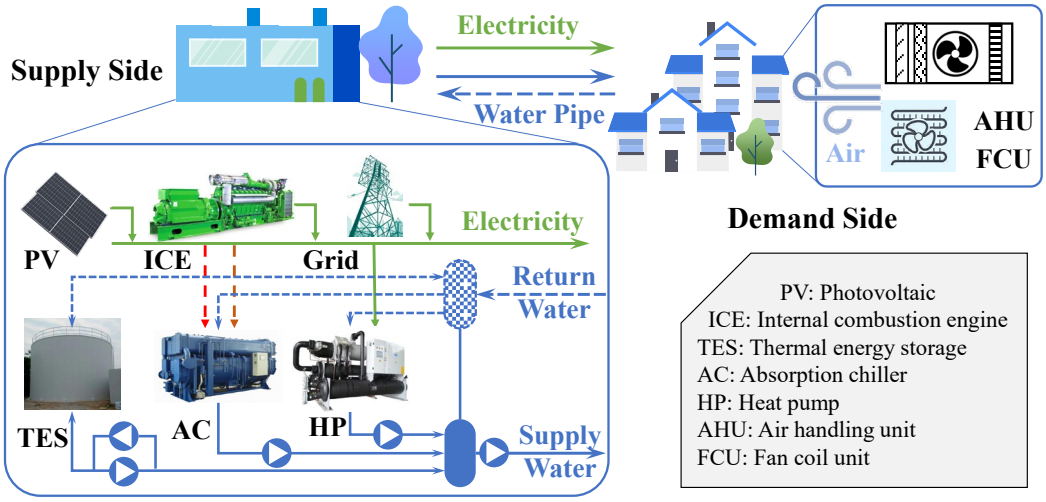

Fig. 3 Configuration of the distributed energy system

Based on the system configuration, the system is modeled in TRNSYS and the models of the main components are introduced in this section.

(1) Internal combustion engine

The internal combustion engine (ICE) model calculates the consumed natural gas and the waste heat generated by inputting the electricity load, which is modeled based on Type 907 in TRNSYS. A detailed description of the model can be found in reference [46]. The required energy supplied by natural gas is calculated by the efficiency and the expected electricity generation. As shown in Eq. (9)–(10), Where, $P_{\mathrm{ICE,out}}$ is the expected power output, $P_{\mathrm{ICE,sha}}$ is shaft power, η_{mec} is mechanical efficiency and η_{ele} is electricity efficiency. Then, after determining the operation status of the unit, the generated waste heat in the jacket water Q_{jw} and the exhaust gas Q_{exh} is calculated in Eq. (11)–(12). f_{jw} and f_{exh} are the proportion of the heat in the jacket water and the exhaust gas to the total exhaust heat, which is given 0.302 and 0.451 respectively at the

rated condition. Based on the calculated energy of the waste heat, the outlet temperature of the jacket water $T_{\text{jw.out}}$ and the exhaust gas $T_{\text{exh.out}}$ can be calculated in Eq. (13)–(14). Where, $T_{\text{jw.in}}$, C_p and $F_{\text{jw.rate}}$ are the inlet temperature, thermal capacity and rated flow rate of the jacket water. $T_{\text{exh.in}}$, $C_{p.\text{exh}}$, $F_{\text{exh.rate}}$ and Fac_{exh} are the inlet temperature, thermal capacity, rated flow rate and flow rate correction factor of the exhaust gas. Under the partial load ratios, the efficiency and waste heat ratio of the ICE will change, which is realized through different coefficients. The coefficients of the ICE model under different load ratios are fitted based on the performance curve, which are shown in Table A1.

$$Q_{\text{re}}=P_{\text{ICE,sh}}/\eta_{\text{ele}} \tag{9}$$

$$P_{\text{ICE,sha}}=P_{\text{ICE,out}}/\eta_{\text{mec}} \tag{10}$$

$$Q_{\text{jw}}=f_{\text{jw}}\times(Q_{\text{re}}-P_{\text{ICE,sha}}) \tag{11}$$

$$Q_{\text{exh}}=f_{\text{exh}}\times(Q_{\text{re}}-P_{\text{ICE,sha}}) \tag{12}$$

$$T_{\text{jw.out}}=T_{\text{jw.in}}+Q_{\text{jw}}/(C_p\times F_{\text{jw.rate}}) \tag{13}$$

$$T_{\text{exh.out}}=T_{\text{exh.in}}+Q_{\text{exh}}/(C_{p.\text{exh}}\times F_{\text{exh.rate}}\times \text{Fac}_{\text{exh}}) \tag{14}$$

(2) Photovoltaic

The photovoltaic (PV) model Type 190 in TRNSYS is used, which is proposed by DeSoto et al [47]. In this model, the current-voltage (I-V) curve of the PV array is determined by five parameters and changes with both insulation and array temperature. A description of the model is detailed in reference [46]. The current-voltage equation is expressed as Eq. (15)–(17). Where, I_L is the light current, I_o is the diode reverse saturation current, R_s is the series resistance, R_{sh} is the shunt resistance and a is the modified ideality factor. Factor a is calculated by the number of individual cells in series N_s, diode ideality factor n_I, Boltzmann constant k, module temperature T_c and electron charge constant q. On the operating conditions, parameters a, I_o, I_L and R_{sh} are modified based on Eq. (18)–(21). R_s is assumed constant at its reference value. In

this study, the value of the five parameters I_L, I_o, R_s, R_{sh} and a are 5.417 A, 1.104×10^{-9} A, 0.5195 Ω, 161 Ω and 1.976, respectively.

$$I=I_L-I_o(e^{(\frac{V+IR_s}{a})}-1)-\frac{V+IR_s}{R_{sh}} \quad (15)$$

$$a=(N_s n_I k T_c)/q \quad (16)$$

$$a/a_{\text{ref}}=T_c/T_{c,\text{ref}} \quad (17)$$

$$\frac{I_o}{I_{o,\text{ref}}}=\left(\frac{T_c}{T_{c,\text{ref}}}\right)^3 exp\left[\frac{1}{k}\left(\frac{E_g}{T}\Big|_{T_{\text{ref}}}-\frac{E_g}{T}\Big|_{T_c}\right)\right] \quad (18)$$

$$\frac{E_g}{E_{g,\text{Tref}}}=1-0.0002677(T-T_{\text{ref}}) \quad (19)$$

$$I_L=\frac{S}{S_{\text{ref}}}\frac{M}{M_{\text{ref}}}\left(I_{L,\text{ref}}+\alpha_{Isc}\left(T_c-T_{\text{c,ref}}\right)\right) \quad (20)$$

$$\frac{R_{sh}}{R_{sh,\text{ref}}}=\frac{S_{\text{ref}}}{S} \quad (21)$$

(3) Absorption chiller

The temperature of the supply water of the ACs is calculated by inputting the temperature and flow rate of the jacket water and the exhaust gas. The model builds on our previous work [26]. Firstly, the input waste heat energy is used to calculate the part load ratio of the input energy plr_{heat} as shown in Eq. (22). Then the COP is modified for the first time under the PLR condition (Eq. (23)). The COP is modified secondly by the β and γ under different chilled water outlet temperature and cooling water inlet temperature as shown in Eq. (24)–(26). Where, $T_{\text{chw,AC,out}}$ and $T_{\text{cw,AC,in}}$ are chilled water outlet temperature and cooling water inlet temperature. a_1–c_3 are coefficients used to describe the characteristics of the polynomial, obtained by fitting the sample parameters. Thirdly, based on the COP and the input heat energy under the operating conditions, the maximum cooling capacity of the AC can be calculated in Eq. (27). In the final step, the needed energy of the chilled water is calculated in Eq. (28) by the thermal capacity C_p, water flow rate $F_{\text{chw,AC}}$, chilled water outlet temperature $T_{\text{chw,AC,out}}$ (assumed to be the set temperature) and chilled water inlet temperature $T_{\text{chw,AC,in}}$. If the needed energy of the chilled water is higher than the maximum cooling capacity of the AC, the outlet temperature of the chilled water is recalculated and the

COP needs to be re-modified until it converges. The coefficients in the model are fitted based on the performance curve of an absorption chiller, which are shown in Table A2.

$$\mathrm{plr}_{heat}=(Q_{exh}+Q_{jw})/(Q_{exh.rate}+Q_{jw.rate}) \quad (22)$$

$$\mathrm{COP}_{plr}=(a_1\times\mathrm{plr}_{heat}^3+a_2\times\mathrm{plr}_{heat}^2+a_3\times\mathrm{plr}_{heat}+a_4)\times Q_{chw.AC}^{rated}/(Q_{exh}+Q_{jw}) \quad (23)$$

$$\beta=b_1\times T_{chw,AC,out}^2+b_2\times T_{chw,AC,out}+b_3 \quad (24)$$

$$\gamma=c_1\times T_{cw,AC,in}^2+c_2\times T_{cw,AC,in}+c_3 \quad (25)$$

$$\mathrm{COP}_{AC}=\mathrm{COP}_{plr}\times\beta\times\gamma \quad (26)$$

$$Q_{chw.AC}^{max}=(Q_{exh}+Q_{jw})\times\mathrm{COP}_{AC} \quad (27)$$

$$Q_{chw,AC}=C_p\times F_{chw,AC}\times(T_{chw,AC,in}-T_{chw,AC,out}) \quad (28)$$

(4) Heat pump

The electricity consumption of the HP is calculated according to the required cooling demand based on the HP model in reference [48]. Firstly, the outlet temperature of the chilled water $T_{chw,HP,out}$ is assumed to be the temperature setpoint and the needed cooling energy $Q_{chw,HP}$ is calculated in Eq. (29). Where, C_p is the thermal capacity of water and $F_{chw.HP}$ is the chilled water flow rate of the HP. The PLR of the HP is then calculated based on the cooling energy and the full capacity CAP_{full}, as shown in Eq. (30). If the calculated PLR is larger than 1, the chilled water outlet temperature is recalculated to keep the cooling energy within the capacity. The electricity consumption of the HP is modified by the chilled water supply water temperature $T_{chw,HP,out}$, cooling water return temperature $T_{cw,HP,in}$ and PLR as shown in Eq. (31)–(34). Parameters with *noc* subscript are indicated to be parameters at nominal conditions. Detailed description of the model is introduced in reference. The coefficients in the HP model e_1–g_3 are adjusted based on performance data, which are fitted based on the performance curve of a heat pump as shown in Table A3.

$$Q_{chw,HP}=C_p\times F_{chw.HP}\times(T_{chw,return}-T_{chw,HP,out}) \quad (29)$$

$$\mathrm{plr}=Q_{\mathrm{chw,HP}}/\mathrm{CAP}_{\mathrm{full}} \tag{30}$$

$$P=P_{\mathrm{noc}}\times\mathrm{CAPFT}\times\mathrm{EIRFT}\times\mathrm{EIRFPLR} \tag{31}$$

$$\mathrm{CAPFT}=\mathrm{CAP}_{\mathrm{full}}/\mathrm{CAP}_{\mathrm{noc}}=e_1+e_2\times(T_{\mathrm{chw,HP,out}}/T_{\mathrm{chw,HP,out,noc}})$$

$$+e_3\times(T_{\mathrm{cw,HP,in}}/T_{\mathrm{cw,HP,in,noc}}) \tag{32}$$

$$\mathrm{EIRFT}=(P_{\mathrm{full}}/\mathrm{CAP}_{\mathrm{full}})/(P_{\mathrm{noc}}/\mathrm{CAP}_{\mathrm{noc}})=f_1$$

$$+f_2\times(T_{\mathrm{chw,HP,out}}/T_{\mathrm{chw,HP,out,noc}})+f_3\times(T_{\mathrm{cw,HP,in}}/T_{\mathrm{cw,HP,in,noc}})$$

$$+f_4\times(T_{\mathrm{chw,HP,out}}/T_{\mathrm{chw,HP,out,noc}})^2+f_5\times(T_{\mathrm{cw,HP,in}}/T_{\mathrm{cw,HP,in,noc}})^2 \tag{33}$$

$$\mathrm{EIRFPLR}=\mathrm{P}/\mathrm{P}_{\mathrm{full}}=g_1\times\mathrm{plr}^2+g_2\times\mathrm{plr}+g_3 \tag{34}$$

(5) Chilled water coil

The model of the chilled water coil is used in the fan coil unit and the air handling unit for the heat exchange between air and water. The chilled water coil model (Partially Wet) Type 124 in TRNSYS is used, which is detailed introduced in reference [46]. The heat transfer rate Q_{AHU} is calculated by the enthalpy-based overall heat transfer coefficient UA_h and the difference between outlet air enthalpy h_{out} and inlet air enthalpy h_{in} as shown in Eq. (35) and (36). After that, the design U-factor times Area (UA) values of the coil need to be determined, as shown in Eq. (37)–(41). Where, $\mathrm{UA}_{\mathrm{ext,rated}}$ and $\mathrm{UA}_{\mathrm{int,\,rated}}$ are rated UA values for the air side and liquid side. Under the operating conditions, the $\mathrm{UA}_{\mathrm{ext}}$ and $\mathrm{UA}_{\mathrm{int}}$ values are adjusted for the inlet conditions. Then, Where, C_p is the specific heat, m_{air}, $T_{\mathrm{air,in}}$, m_{liq}, $T_{\mathrm{liq,in}}$ are the flow rate and inlet temperature of the air and fluid on the operating conditions.

$$Q_{\mathrm{AHU}}=\mathrm{UA}_h\times(h_{\mathrm{out}}-h_{\mathrm{in}}) \tag{35}$$

$$\mathrm{UA}_h=\mathrm{UA}/C_p \tag{36}$$

$$UA=1/(1/(UA_{ext})+1/(UA_{int})) \quad (37)$$

$$UA_{ext}=UA_{ext,rated}\times x_a \times(m_{air}/m_{air,rated})^{0.8} \quad (38)$$

$$x_a=1+0.004769\times(T_{air,in}-T_{air,in,rated}) \quad (39)$$

$$UA_{int}=UA_{int,rated}\times x_w \times(m_{liq}/m_{liq,rated})^{0.85} \quad (40)$$

$$x_w=1+(0.014/(1+0.014\times T_{liq,in,rated}))\times(T_{liq,in}-T_{liq,in,rated}) \quad (41)$$

(6) Water pipe

The water pipe model is used to describe the temperature transmission delay characteristics and energy storage characteristics of the chilled water system in the DES. The pipe model Type 31 in TRNSYS is used [46]. The outlet temperature of the pipe is given by Eq. (42). Where $\dot{m}$ is the mass flow rate of liquid through the pipe, Δt is the simulation time step, M is the total mass of water contained in the pipe, j and k are subscripts used to denote liquid segments. The coefficient n and the subscript k must satisfy the conditions shown in Eq. (43)–(44). The energy loss of the pipe is calculated based on the resistances of the pipe (R_{inside}, R_{pipe}, R_{insul} and $R_{outside}$) and the temperature difference between the liquid T_j and the environment T_{env} as shown in Eq. (45). The energy stored in the pipe can be calculated by the total mass of water and the temperature difference as shown in Eq. (46).

$$T_{out}=1/\dot{m}\Delta t\times\sum_{j=1}^{k-1}(M_jT_j+nM_kT_k) \quad (42)$$

$$0\le n\le 1 \quad (43)$$

$$\sum_{j=1}^{k-1}(M_j+nM_k)=\dot{m}\Delta t \quad (44)$$

$$M_jC_p\frac{dT_j}{dt}=-\left(\frac{1}{R_{inside}+R_{pipe}+R_{insul}+R_{outside}}\right)_j(T_j-T_{env}) \quad (45)$$

$$\Delta E=MC_p(\bar{T}_f-T_{initial}) \quad (46)$$

2.4 Performance evaluation criteria

To quantify the system operation performance, the cooling utilization ratio, part load ratio and primary energy efficiency are used. The cooling utilization ratio CUR_{AC}

under the current waste heat input is used to evaluate whether the ACs achieve maximum cooling output by fully utilizing waste heat. As shown in Eq. (47) [26], $\mathrm{CUR_{AC}}$ is the ratio of the produced cooling energy $Q_{\mathrm{chw.AC}}$ to the maximum produced cooling energy based on the current available waste heat $Q_{\mathrm{chw.AC}}^{\mathrm{max}}$. The maximum value of this criterion is 1, indicating that the AC makes better use of the waste heat for cooling. The part load ratio of the absorption chiller $\mathrm{PLR_{AC}}$ and the heat pump $\mathrm{PLR_{HP}}$ is the ratio of the produced cooling energy $Q_{\mathrm{chw.AC}}$ and $Q_{\mathrm{chw.HP}}$ to the rated capacity $Q_{\mathrm{chw.AC}}^{\mathrm{rated}}$ and $Q_{\mathrm{chw.HP}}^{\mathrm{rated}}$, as shown in Eq. (48)–(49) [26]. The primary energy efficiency PEE is calculated in Eq. (50) [9], in which the E_{ICE} is the electricity generated by the ICE, Q_{re} is the energy of the consumed natural gas. The operation cost OC (Eq. (51) [9]) contains the energy cost by ICE, electricity bills and system maintenance cost. The carbon emission CE is calculated based on Eq. (52) [9] for the environmental analysis, which contains carbon emissions from the consumed natural gas and indirect carbon emissions from the grid.

$$\mathrm{CUR_{AC}}=\frac{Q_{\mathrm{chw.AC}}}{Q_{\mathrm{chw.AC}}^{\mathrm{max}}} \tag{47}$$

$$\mathrm{PLR_{AC}}=\frac{Q_{\mathrm{chw.AC}}}{Q_{\mathrm{chw.AC}}^{\mathrm{rated}}} \tag{48}$$

$$\mathrm{PLR_{HP}}=\frac{Q_{\mathrm{chw.HP}}}{Q_{\mathrm{chw.HP}}^{\mathrm{rated}}} \tag{49}$$

$$\mathrm{PEE}=\frac{E_{\mathrm{ICE}}+Q_{\mathrm{chw.AC}}}{Q_{\mathrm{re}}} \tag{50}$$

$$\mathrm{OC}=V_{\mathrm{gas}}\cdot Pc_{\mathrm{gas}}+P_{\mathrm{grid}}\cdot Pc_{\mathrm{grid}}+P_{\mathrm{ICE}}\cdot Pc_{\mathrm{maint}} \tag{51}$$

$$\mathrm{CE}=V_{\mathrm{gas}}\cdot \vartheta_{\mathrm{gas}}+E_{\mathrm{grid}}\cdot \vartheta_{\mathrm{grid}} \tag{52}$$

3 Results and discussion

In this section, the performance of the DES under the conventional and the proposed strategy is analyzed under different electricity and cooling loads. Then the performance of the DES under the proposed F-method and T-method on a typical summer day is analyzed and compared with different water systems. Finally, the effectiveness of the proposed methods under different scenarios is studied by changing the PV power

contributions and indoor temperature setpoint.

3.1 System description

A campus in hot summer and cold winter area in China is selected to study the performance of DES. Four types of buildings with different characteristics are considered: office buildings, classroom buildings, dormitories and residential buildings. The gross area of the buildings is around 478600 m^2 and the air conditioning area accounts for 70%. The load of each type of building is calculated. The office building accounts for 56.5% of the total building load and followed by the residential (17.9%) and the dormitory (17.6%). The annual electricity, heating and cooling loads are shown in Fig. 4. The maximum cooling load is 55270 kW. In a typical summer week, the cooling and electricity load is higher during the day. With a certain proportion of residential buildings, the cooling load at night is much higher than the electrical load. Based on the load, the system can be designed.

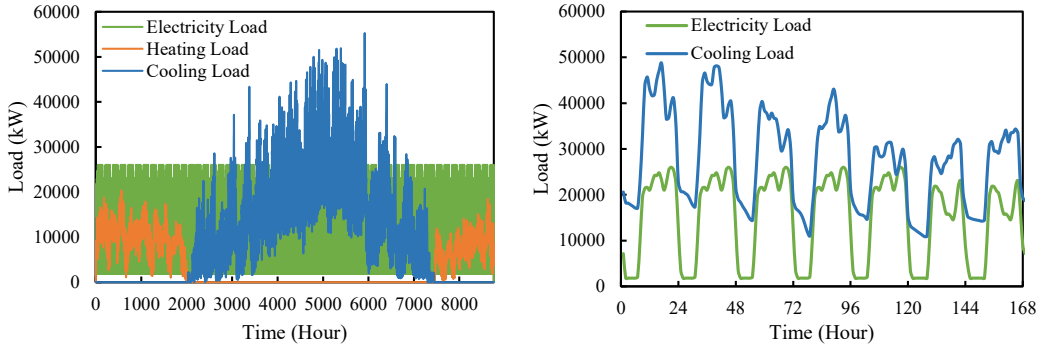

(a) Annual load (b) Load in a typical summer week

Fig. 4 Electricity, Cooling and heating load of the DES

The system information is shown in Table 1. Three ICEs with 9500 kW are selected. The PV is selected based on the total roof area. Three absorption chillers of 7400 kW and four heat pumps of 7735 kW are used to meet the cooling load. On the user side, each type of building is represented by a room model with corresponding air-handling equipment. In the case study, Pc_{gas}, Pc_{grid} and Pc_{maint} used in the economic performance analysis are 2.5 CNY/Nm^3, 0.6 CNY/kWh and 0.1 CNY/kWh,

490 respectively. In environmental analysis, ϑ_{gas} and ϑ_{grid} are 1.96 t/MJ and 0.581 t/MWh,
491 respectively [49].

492 Table 1 System design parameters

Variable	Value
Internal combustion engine	
Capacity	9500 kW
Number	3
Photovoltaic	
Voltage at max power point and reference conditions	35.7 V
Current at max power point and reference conditions	4.9 A
Module area	0.89 m^2
Number of modules	111335
Absorption chiller	
Capacity	7400 kW
Number	3
Coefficient of performance	1.1
Rated cooling source flow rate	907 kg/s
Rated cooling load flow rate	252 kg/s
Heat pump	
Capacity	7735 kW
Number	4
Rated cooling cop	5.77
Rated cooling power	1340 kW
Rated cooling source flow rate	435 kg/s
Rated cooling load flow rate	264 kg/s

493 ## 3.2 Assessment of the conventional and proposed load allocation methods

494 To illustrate the operation problem of the DES under the conventional load allocation
495 method and the improvement of the proposed load allocation method, the system
496 operation status and energy utilization efficiency are evaluated by changing the cooling
497 load under different electricity load.

498 (1) Conventional load allocation method

499 Under the conventional load allocation method, the primary water flow rate is typically
500 constant. The performance of the DES under the conventional load allocation method
501 was evaluated to illustrate the operation deviation problem in the DES. Fig. 5 shows

the primary energy efficiency (PEE) of the DES and flow rates of the ACs and HPs under different electricity and cooling loads. When the electricity load of the system was 100%, as the cooling load decreased, the water flow on the user side decreased, and the number of HPs gradually decreased. The ACs operated following the ICE; therefore, the open number and flow rate of the ACs remained constant. However, the PEE gradually decreased with a decrease in the flow rate on the user side and increased when one HP was turned off. This phenomenon indicated that the ACs were affected by the operation of the HPs and did not follow the operation of the ICEs well. This is inconsistent with the expectations of the operation strategy. The absorption unit did not fully utilize the waste heat for cooling. When the HPs were in operation, the PEE decreased to 68%. When all the HPs were shut down, the PEE gradually decreased to 55%. This phenomenon also occurred when the electricity load decreased to 75%, 50%, and 25%. When the electricity load decreased to 50%, only one AC was opened, and the influence of the load on the PEE increased. The lowest PEE value decreased to 64% when the HPs were operated. In contrast, when the electrical load was further reduced to 25%, the impact of the load changed, and the number of HPs with the PEE was reduced. The PEE exceeded 81% when two HPs were on. The results showed that the changes in the load and number of HPs would deteriorate the operation of the ACs without considering the control of the water system under the conventional load allocation method. This system operation deviation problem reduced the waste utilization ratio and PEE of the DES. This effect was greater when fewer ICEs and ACs were operated. The results demonstrate the need for an improved load distribution method that allows the system to efficiently use waste heat and improve the PEE under different load conditions.

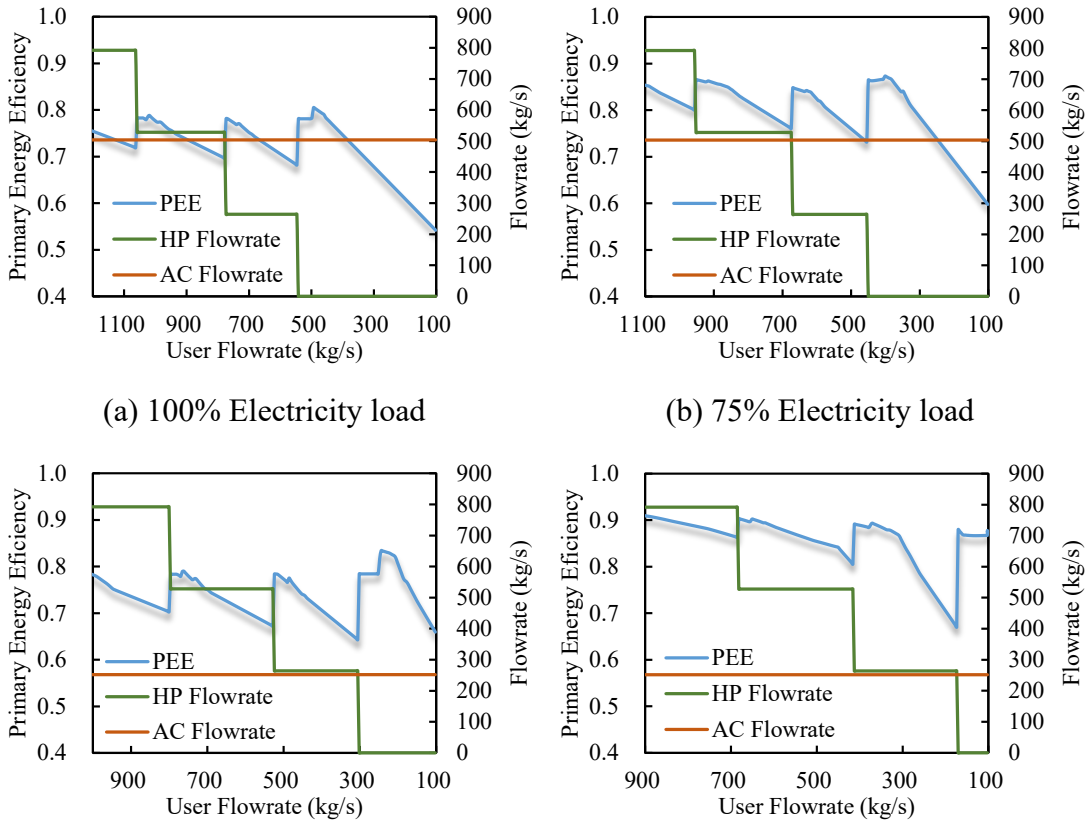

(a) 100% Electricity load (b) 75% Electricity load

(c) 50% Electricity load (d) 25% Electricity load

Fig. 5 Performance state for DES under constant flow water system

The part load ratios of the ACs and HPs were analyzed. The cooling utilization ratio (CUR), supply water temperature (T divider), and return water temperature (T collector) were used, as shown in Fig. 6. The supply water temperature was set to 6 ℃, and the return water temperature changed with the cooling load. When the cooling load decreased, the user flow rate and return water temperature decreased. Because the ratio of the cooling production of the ACs and HPs was constant in the conventional load allocation method, the part load ratio (PLR) of both the HPs and ACs decreased, resulting in a decline in the CUR and PEE. When the electricity load decreased to 50% and only one AC was operated, as shown in Fig. 6(c), the last HP shut down until the PLR of the HP and AC decreased to nearly 60%, considerably influencing the PEE. When the electricity load decreased to 25%, considerably less waste heat from the ICE could be used; therefore, the AC operated at a low PLR. Therefore, the influence of the HPs on the ACs was smaller, and the CUR was 1 in

most states, indicating that the waste heat from the ICEs could be efficiently used by the ACs. In other words, in the conventional load allocation method, because of the fixed proportion of cooling from the AC and HP, the HP affected the operation of the AC under a changing load. This influence could prevent the ACs from following the ICEs well, resulting in a low energy utilization ratio that must be addressed by water system controls in load allocation methods.

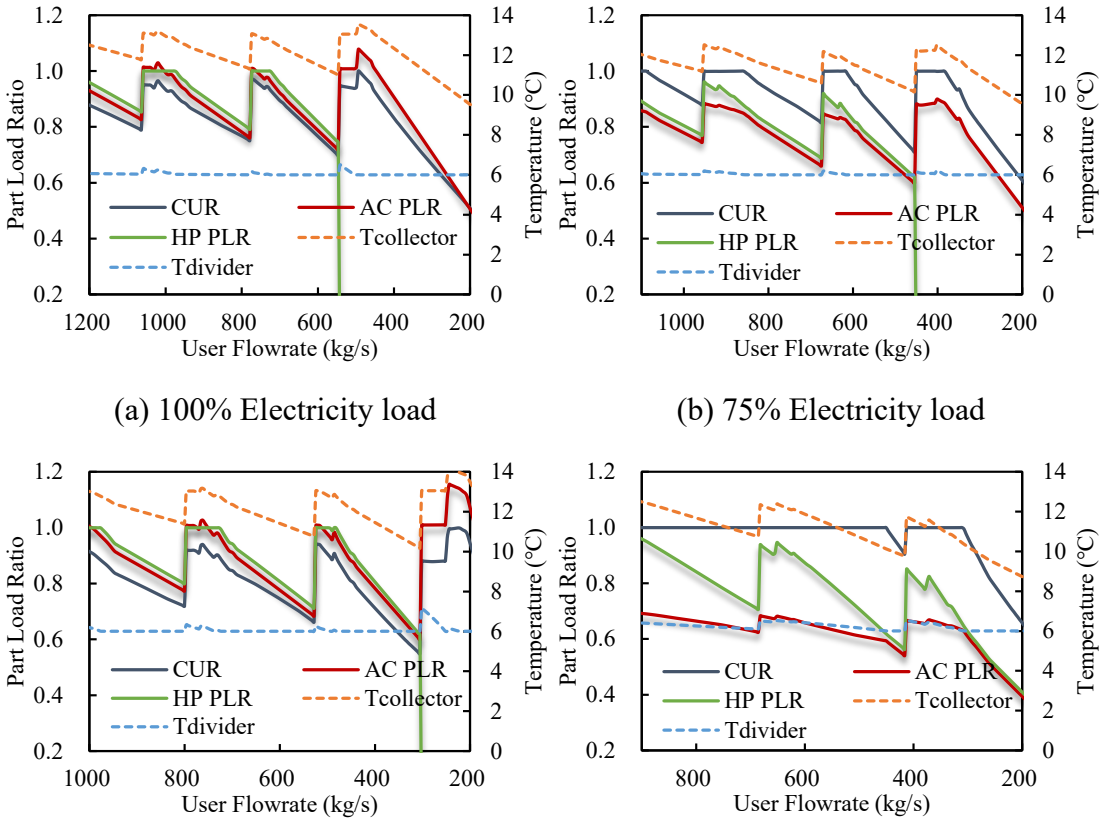

(a) 100% Electricity load (b) 75% Electricity load

(c) 50% Electricity load (d) 25% Electricity load

Fig. 6 Operating state for DES under constant flow water system

(2) Proposed load allocation method

To prevent the DES from deviating from the operation strategies, a load allocation method that adjusts the flow rate (F-method) and supply temperature (T-method) of the HPs was proposed to allocate the load between the ACs and the HPs. For the variable flow rate systems, the F-method was used to adjust the flow rates of the ACs and HPs. The performance of the DES under the F-method is shown in Fig. 7. The flow rate of

the ACs was adjusted based on the maximum cooling production. Because the electricity load was unchanged in this assessment, the amount of waste heat and flow rate of the AC were stable when the HPs were operating. With a decrease in the user load, the flow rate of the HP gradually decreased, enabling the ACs to operate following the waste heat. In this method, the PEE of the DES was high when the HPs were opened, indicating that the ACs could operate following the ICEs without being affected by the load and HPs. When all HPs were shut down, the PEE still decreased with a reduction in the cooling load because significant cooling energy was not required. Thermal energy storage systems are required to store the surplus energy to further increase the PEE in this situation. From the PLR curves, with a decrease in the user flow rate, the PLR of the HP changed, but its influence on the AC was eliminated. The CUR remained at 1, indicating that the ACs could fully utilize the waste heat. The results indicated that the proposed F-method was effective in ensuring that the AC followed the waste heat well and improved the system performance.

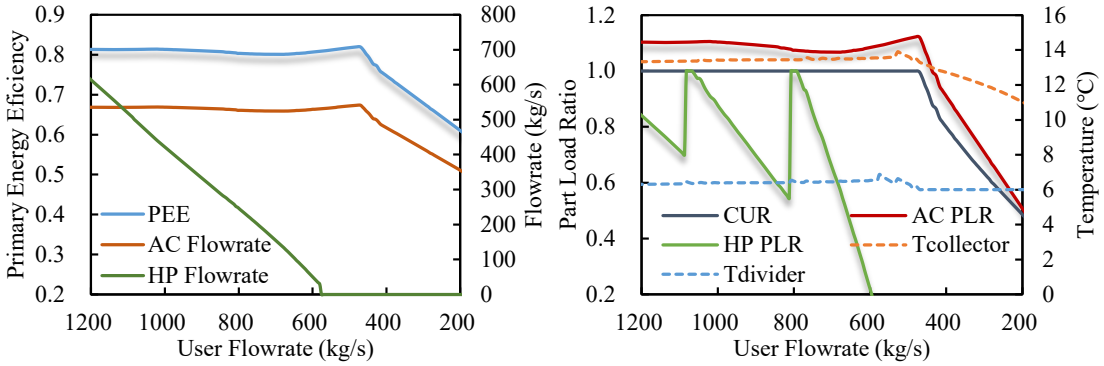

(a) System efficiency and flow rate (b) Device PLR and temperature

Fig. 7 Performance for DES under the F-method

For the DES with a constant flow rate system, the flow rates of the ACs and HPs were unchanged; however, the supply water temperature of the HP was adjusted using the T-method. As shown in Fig. 8, the temperature of the supply water changed between 6 and 8 ℃. As the cooling load decreased, the PLR of the HP changed, but the AC followed the waste heat well. Hence, the CUR and PLR of the AC did not change significantly, indicating that the waste heat could be fully used. Therefore, the system

PEE was always higher than 0.8 when the HPs were open; this was considerably more stable and higher than that under the conventional load allocation method. The results showed that adjusting the supply water temperature of the HPs could improve the system energy utilization efficiency by ensuring that the ACs followed the ICEs well, as expected, without exposure to the load and HPs.

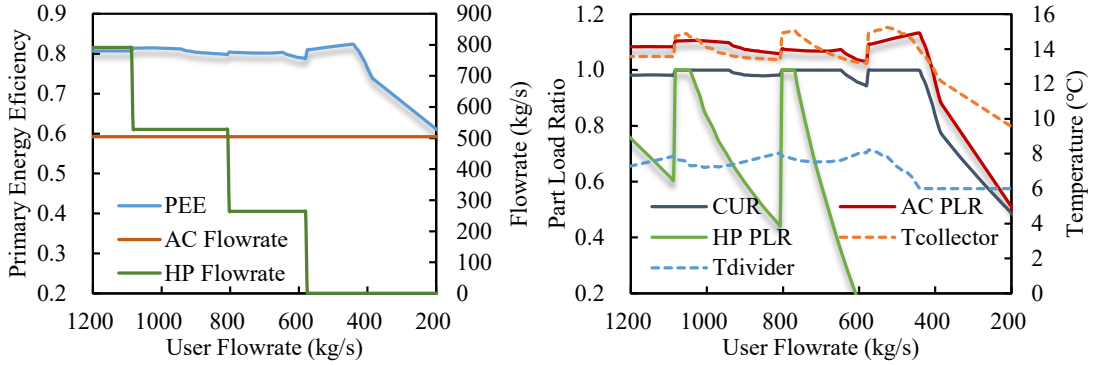

(a) System efficiency and flow rate (b) Device PLR and temperature

Fig. 8 Performance for DES under the temperature adjustment method

3.3 System performance comparison under different load allocation methods

The system performance under the proposed load allocation method is studied on typical days and compared with different allocation methods. The constant primary water flow rate (Scenario 1), variable primary water flow rate of ACs (Scenario 2) and variable primary water flow rate of HPs (Scenario 3) are selected as shown in Table 2. The proposed load allocation method to adjust the flow rate (F-method) and the supply temperature (T-method) is compared in Scenario 4 and Scenario 5.

Table 2 Scenario settings

Scenario	Water Flow Rate		Supply Temperature	
	Absorption Chiller (AC)	Heat Pump (HP)	Absorption Chiller	Heat Pump
1. Constant	Rated	Rated	6℃	6℃
2. Variable HP	Rated	Vary with PLR	6℃	6℃
3. Variable AC	Vary with PLR	Rated	6℃	6℃
4. F-method	Vary with PLR	Calculated	6℃	6℃
5. T-method	Rated	Rated	6℃	Calculated

(1) System performance under the proposed load allocation method

The daily operation of the DES under the proposed load allocation method was analyzed. The electricity and cooling balance of the DES under the F-method is shown in Fig. 9. The PV and ICE were equipped to satisfy the electricity load of the user and electricity consumption of the cooling system (HP, water pump, and fan). Insufficient electricity was purchased from the grid The ICE supplied most of the total electricity load during the entire day, and the peak contribution of the PV reached 14 MW at midday. Regarding the cooling balance, the cooling load reached a maximum value of 48.8 MW at around 14:00. The ACs produced cooling energy using the waste heat from the ICEs, and the insufficient part was satisfied by the HPs. The system temperature and flow rate in Scenario 4 are shown in Fig. 10. In the F-method, the water flow rates of the ACs and HPs were adjusted according to the operating conditions. The supply water temperature was maintained at set point (6 °C), except in the morning when the load increased rapidly. The CUR of the ACs was maintained at 1, indicating that the waste heat was fully used under the F-method.

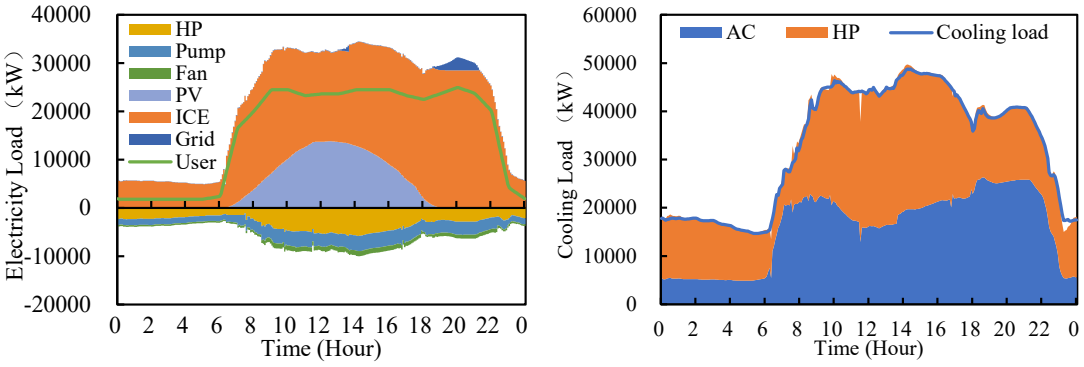

(a) Electricity balance (b) Cooling balance

Fig. 9 Electricity and cooling balance of DES in scenario 4 (F-method)

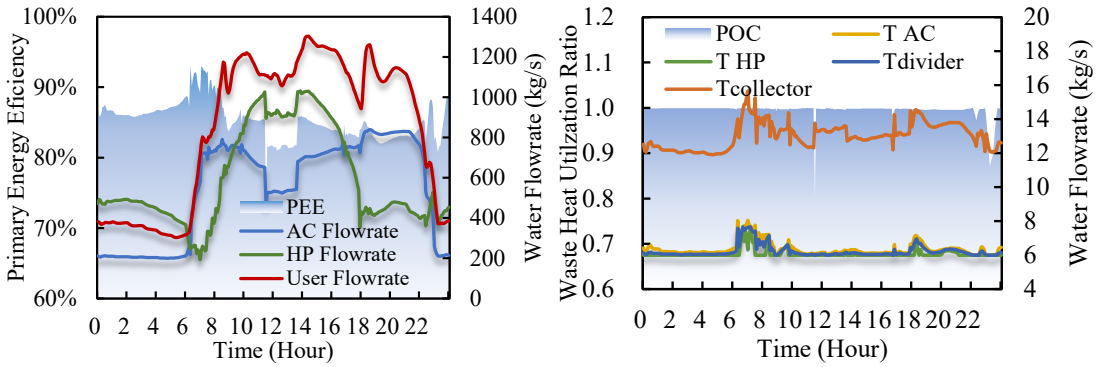

(a) System efficiency and flow rate (b) Device CUR and temperature

Fig. 10 Temperature and flow rate of DES in scenario 4 (F-method)

The operation of the DES in Scenario 5 was similar; however, in the T-method, the flow rates of the ACs and HPs were constant. The supply water temperature of the HPs was adjusted by varying the load. As shown in Fig. 11, the temperature of the divider varied between 5.6–8.2 ℃. Except for the temporary temperature increase in the morning, the highest supply temperature was 7.4 ℃. The higher temperature resulted from the higher supply temperature of the HPs; this reduced the cooling load of the HPs and enabled the ACs to use more waste heat to produce more cooling energy. Under the T-method, a POC of almost 1 indicated that the ACs could also fully utilize the waste heat. The increased supply temperature of the HPs was beneficial to their COP. However, with the increase in the supply water temperature, the flow rate of the user increased, thus increasing the power consumption of the water pumps.

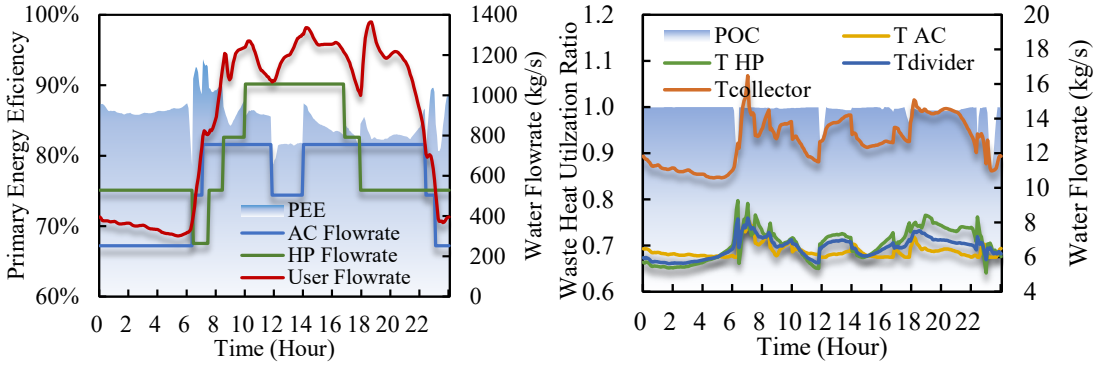

(a) System efficiency and flow rate (b) Device CUR and temperature

Fig. 11 Temperature and flow rate of DES in scenario 5 (T-method)

(2) Comparison between different load allocation methods

A comparison of the PEE and CUR in the five scenarios is shown in Fig. 12. The CUR of S3 was the lowest during most periods. The CUR of the system using the proposed strategies (S4 and S5) was the highest. The CUR was maintained at 1, indicating that the waste heat was utilized well under the proposed method. As noted from the PEE curves, scenarios with a higher CUR typically had a higher PEE. S4 and S5 had the highest PEE values for most of the daytime. The results showed that the proposed method could achieve a better system PEE by improving waste heat utilization.

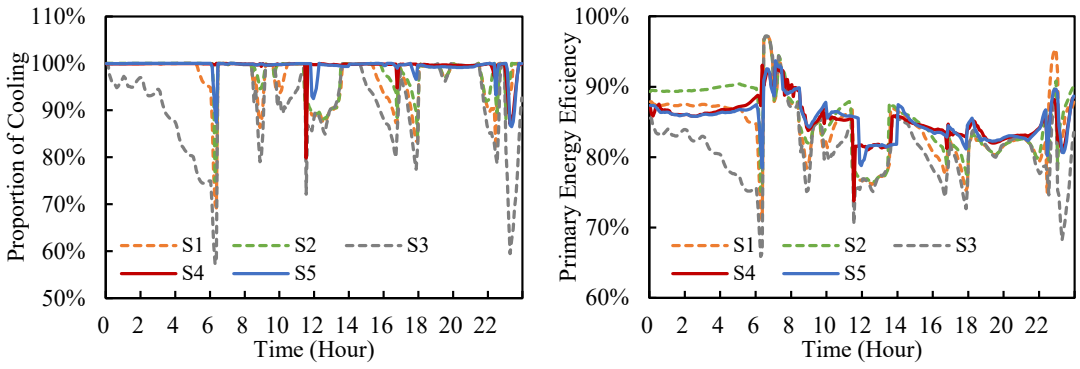

(a) Cooling utilization ratio (b) Primary energy efficiency

Fig. 12 CUR and PEE comparison under five scenarios

The daily average energy performances are listed in Table 3. From an energy perspective, the total cooling loads in the five scenarios were almost the same, but the cooling energy supplied by the ACs was low in the first three scenarios. This implied that the waste heat was not fully used by the ACs; therefore, an insufficient part of the load had to be met by the HPs, resulting in higher HP power consumption. In the DES, where only the flow rate of the HP was adjusted by the PLR (S3), the ACs provided a lower proportion of cooling energy (44.47%), indicating that the waste heat utilization ratio was low in this scenario. The AC CUR in S4 and S5 were considerably higher; therefore, the cooling energy provided by the AC was the highest (383 and 382 MWh), and the daily average PEE was also the highest (84.67% and 84.68%, respectively). Owing to the higher cooling production of the ACs under the proposed load allocation

658 method (S4 and S5), the consumption of the HP decreased to 76.2 and 74.4 MWh. In
659 S5, when the supply water temperature of the HPs increased, the COP of the HP
660 increased, and the electricity consumption of the HP was the lowest. However, an
661 increase in the supply water temperature increased the power consumption of the water
662 pumps. The consumption of the water pumps in S4 was the lowest because of the lower
663 flow rates of both the ACs and HPs. The total electricity savings of the cooling system
664 were 2.74% and 3.56% in S4 and S5, respectively. The results showed that both the F-
665 and T-methods were effective for improving the system energy performance.

666 Table 3 System energy performance under five scenarios

	S1	S2	S3	S4	S5
AC Cooling (MWh)	371	377	357	383	382
HP Cooling (MWh)	432	427	446	422	422
AC Cooling utilization ratio	46.21%	46.86%	44.47%	47.59%	47.49%
Primary energy efficiency	82.94%	83.73%	81.25%	84.67%	84.68%
HP COP	5.43	5.48	5.39	5.54	5.68
HP Electricity (MWh)	79.5	78.0	82.8	76.2	74.4
Pump Electricity (MWh)	54.8	54.7	54.6	54.0	54.8
Fan Electricity (MWh)	16.0	16.0	15.9	16.0	15.7
Cooling Total Electricity (MWh)	150	149	153	146	145
Cooling Electricity Saving	/	1.12%	-2.04%	2.74%	3.56%

667 The economic and environmental performances under the five scenarios are shown in
668 Fig. 13. Because of the decrease in the energy cost, the operation cost of the DES in S4
669 and S5 could be decreased to approximately 301×10^3 CNY. Compared with S1, the cost
670 savings were 1.31% and 1.55%, respectively. The carbon emissions of the DES
671 exhibited similar trends. Lower carbon emissions occurred in S4 and S5 (204 t and 203
672 t, respectively). By separating the carbon emissions of the cooling systems, the carbon
673 emissions of the cooling systems in S4 and S5 were reduced by 3.36% and 4.21%,
674 respectively. Therefore, the results showed that the proposed load allocation method
675 could reduce the operation costs and carbon emissions by effectively improving the
676 system waste heat utilization rate and energy utilization efficiency.

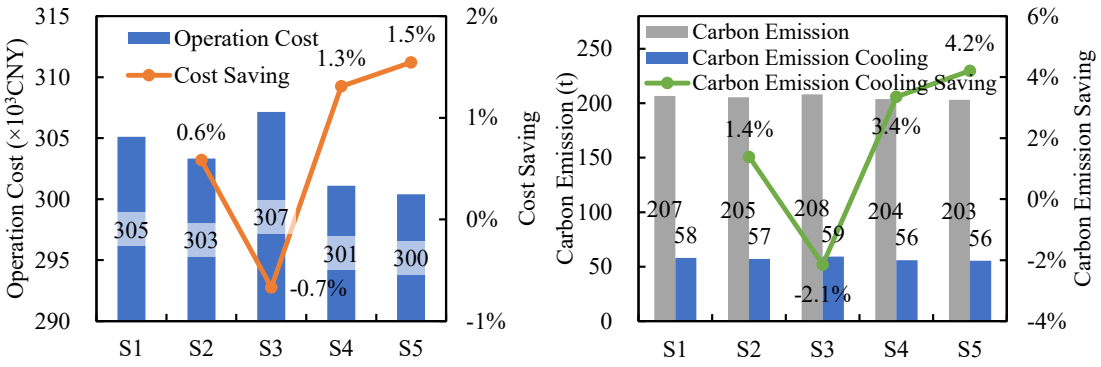

(a) System economic performance (b) System carbon emission

Fig. 13 The economic and environmental performance of the DES under five scenarios

3.4 Load adaptability study of the proposed load allocation method

The electricity load and cooling load of the DES have a great influence on the operation of the system and the effectiveness of the method. Therefore, a load adaptability study is conducted to study the effectiveness of the proposed method under different electricity and cooling scenarios.

(1) Impact of different PV contributions

First, different PV contributions were studied because a PV contributes to more than 19% of the total electricity load and significantly impacts the operation of the ICE and AC. The improvements in the DES under the F- and T-methods under different PV contributions are shown in Fig. 14, considering three cases (PV fully installed, PV 50% installed, and no PV). From an energy performance perspective, when the contribution of the PV decreased, the system PEE under both the T- and F-methods decreased. However, the PEE improvement under the proposed strategy was greater when the PV installation decreased to 50% and 0%. The highest PEE improvement rate achieved was 2.5%. The cost savings also increased under the proposed strategy, and the highest cost savings increased from 1.5% to 2.2%. According to the environmental performance, as shown in Fig. 14 (b), although the total carbon emissions increased with a decrease in the number of PV panels, the improvement was greater compared with that of the DES

under the conventional method. When the PV panels were fully installed, the carbon emission reductions of the cooling system were 3.4% and 4.2% using the F- and T-methods, respectively. When the PV panel was not considered, the carbon emission reduction of the cooling system further increased to 5.8% and 7.7%, respectively. A greater improvement was observed in the lower PV installation ratio because the ICEs produced more electricity and waste heat when fewer PV panels were installed, leading to a greater improvement when the waste heat was fully used.

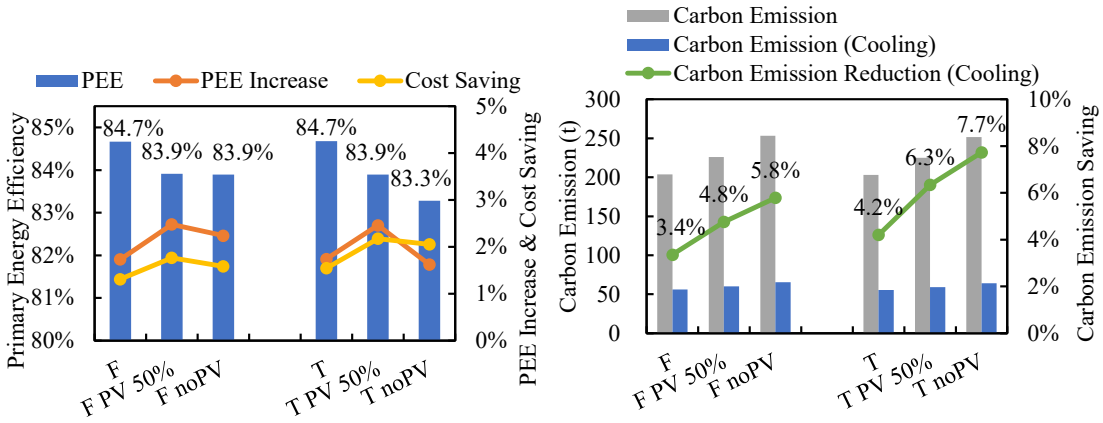

(a) System energy and economic performance (b) System carbon emission

Fig. 14 System performance under different PV contributions

(2) Impact of different indoor temperature

To study the effects of different cooling loads on the proposed method, different indoor temperatures were used to change the cooling loads. As shown in Fig. 15, by increasing the indoor temperature by 1°C (ΔT=1) and 2 °C (ΔT=2), the PEE increased, and the PEE improvement also increased. The improvements in the F- and T-methods– increased from 1.7% to 4.3% and 4.4%, respectively. The cost savings of the two methods also increased by approximately 0.7–0.8%. According to the environmental performance, as shown in Fig. 15 (b), the cooling system carbon emission reduction of the F-method increased from 3.4% to 8.6%. In the T-method, the improvement increased to 7.4% and 8.8% for 1°C and 2°C increase in the indoor temperature, respectively. The results indicated that the proposed methods were more effective when the system cooling load was relatively small. This was primarily because fewer chillers

operated when the cooling load of the system was low. The chillers are easier to operate under low part-load conditions, and more waste heat tends to be wasted without appropriate control. Therefore, using the proposed load allocation methods to fully use the waste heat could achieve a greater improvement under low cooling load conditions.

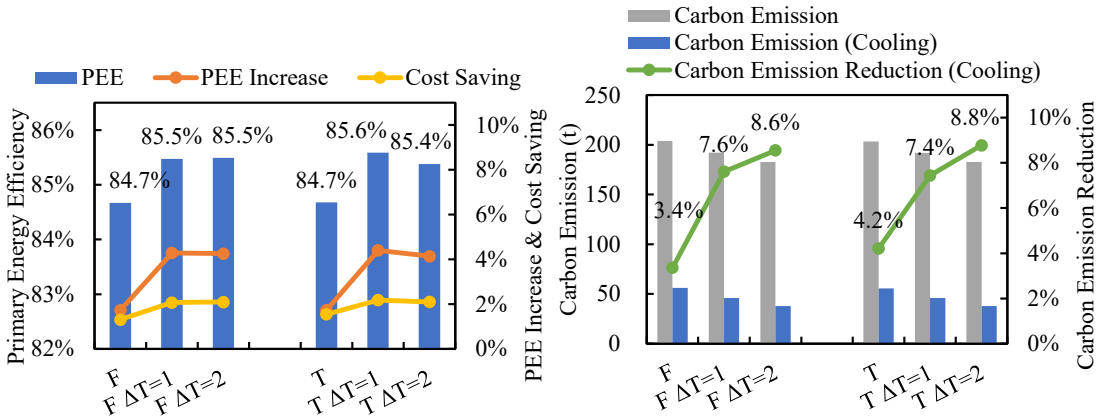

(a) System energy and economic performance (b) System carbon emission

Fig. 15 System performance under different indoor temperatures

3.5 Discussion

In this study, a load allocation method was proposed for DESs to solve the load distribution problem between ACs and electrical chillers/HPs. This method is not a new operation strategy, but a water system control method to ensure that the system runs according to the existing strategy, and cannot be ignored during the operation of the system. Although average load allocation is common in cooling systems with multiple chillers, DESs include waste-heat-driven and electric-driven chillers; the average load allocation implies that in most states, waste heat-driven chillers do not fully utilize the waste heat, and electric-driven chillers consume more electricity. This phenomenon has been proven in the aforementioned studies to have a significant impact on the utilization rate of waste heat, primary energy, and system economy. This problem may be one reason for the low system operation efficiency and unsatisfactory economic performance in DES projects. The proposed method proved to improve the system performance in different situations. This indicated that the poor running state of the system was not entirely a problem with the system operation strategy, but that the

743 system operation deviated from the operation strategy. Therefore, in actual DES
744 projects, the change in the number of chillers, as well as the frequency control or start
745 and stop of the pumps, must be performed more cautiously. Based on the automatic
746 control system, the parameters required for the method can be monitored by the sensors
747 and calculated in the local computer. Then, the water pump and the chillers can be
748 controlled automatically in real time or adjusted intermittently to improve the system
749 performance. However, this study mainly explains the importance of the load allocation
750 problem and feasible solutions. In practical applications, disturbances and uncertainties
751 may exist; therefore, the actual effects of this method must be further tested in practice.

752 # 4 Conclusions

753 To solve the system operation deviation problem of a DES, which is caused by ignoring
754 the water system control between ACs and HPs, this study proposed a load allocation
755 control method between thermal- and electrical-driven chillers/HPs by adjusting the
756 flow rate (F-method) or supply water temperature (T-method) of the HPs to ensure that
757 the DES ran efficiently without deviating from the operation strategy. According to the
758 system analyses based on the case study, the following conclusions were drawn.

759 (1) In DESs with ACs and HPs, the operation of the ACs was affected by the HPs
760 without appropriate chilled water control, preventing the ACs from thoroughly
761 following the power generators; consequently, the PEE decreased to 68%. This
762 impact was greater when fewer ICEs and ACs were operated.

763 (2) The proposed load allocation method ensured that the ACs followed the ICEs well,
764 with a CUR of the ACs close to 1, by controlling the flow rate (F-method) or supply
765 temperature (T-method) of the HPs.

766 (3) The proposed control method increased the system PEE from 82.94% to 84.67%
767 compared with that of a constant flow rate control system. System operation costs
768 and carbon emissions of the cooling systems were reduced by 1.55% and 4.21%,

respectively. Adjusting the outlet temperature of the HPs (T-method) achieved better performance owing to the higher COP of the HPs.

(4) The load adaptability study showed that the proposed methods were more effective when more waste heat was available or when the cooling load was low. The carbon emission reduction of the cooling system increased to 7.7% under more available waste heat, and further increased to 8.8% under a lower cooling load.

The proposed load allocation method can make different types of chillers follow the operation strategy well through the water system control. This paper would provide support for the efficient operation of DESs. Future research may focus on the stability of the method in the presence of multiple disturbances and uncertainties in the practical application environment.

Acknowledgement

The research presented in this paper is supported by the National Key Research and Development Program of China (2021YFE0107400)

Appendix A.

Table A1 Value of coefficients in ICE model under different load ratios

plr	η_{ele}	η_{mec}	f_{jw}	f_{exh}	Fac_{exh}
0.40	0.425	0.989	0.155	0.559	0.398
0.50	0.438	0.996	0.179	0.539	0.474
0.60	0.448	0.997	0.200	0.522	0.559
0.70	0.453	0.996	0.222	0.505	0.653
0.75	0.454	0.992	0.243	0.490	0.716
0.80	0.453	0.988	0.264	0.476	0.782
0.90	0.452	0.984	0.283	0.462	0.887
1.00	0.445	0.980	0.302	0.451	1.000

Table A2 Value of coefficients in absorption chiller model

Coefficients	Value	Coefficients	Value	Coefficients	Value
a_1	1.4196	b_1	-0.01069	c_1	-0.0021
a_2	-3.6846	b_2	0.24992	c_2	0.0911
a_3	3.8314	b_3	-0.22439	c_3	0.2350

a_4	-0.5630				

Table A3 Value of coefficients in heat pump model

Coefficients	Value	Coefficients	Value	Coefficients	Value
e_1	1.0340	f_2	0.01914	g_1	0.8382
e_2	0.2508	f_3	0.00659	g_2	-0.0604
e_3	-0.2848	f_4	-0.09575	g_3	0.2203
f_1	0.58170	f_5	0.49110		

Reference

[1] Li B, You L, Zheng M, Wang Y, Wang Z. Energy consumption pattern and indoor thermal environment of residential building in rural China. Energy and Built Environment 2020;1(3):327-36. https://doi.org/10.1016/j.enbenv.2020.04.004.

[2] Pérez-Lombard L, Ortiz J, Pout C. A review on buildings energy consumption information. Energy and Buildings 2008;40(3):394-8. https://doi.org/10.1016/j.enbuild.2007.03.007.

[3] Wen Q, Liu G, Rao Z, Liao S. Applications, evaluations and supportive strategies of distributed energy systems: A review. Energy and Buildings 2020;225. https://doi.org/10.1016/j.enbuild.2020.110314.

[4] Ren F, Wei Z, Zhai X. A review on the integration and optimization of distributed energy systems. Renewable and Sustainable Energy Reviews 2022;162:112440. https://doi.org/10.1016/j.rser.2022.112440.

[5] Chen X, Xiao J, Yuan J, Xiao Z, Gang W. Application and performance analysis of 100% renewable energy systems serving low-density communities. Renewable Energy 2021;176:433-46. https://doi.org/10.1016/j.renene.2021.05.117.

[6] Zhang C, Xue X, Du Q, Luo Y, Gang W. Study on the performance of distributed energy systems based on historical loads considering parameter uncertainties for decision making. Energy 2019;176:778-91. https://doi.org/10.1016/j.energy.2019.04.042.

[7] Han J, Ouyang L, Xu Y, Zeng R, Kang S, Zhang G. Current status of distributed energy system in China. Renewable and Sustainable Energy Reviews 2016;55:288-97. https://doi.org/10.1016/j.rser.2015.10.147.

[8] Twaha S, Ramli M A M. A review of optimization approaches for hybrid distributed energy generation systems: Off-grid and grid-connected systems. Sustainable Cities and Society 2018;41:320-31. https://doi.org/10.1016/j.scs.2018.05.027.

[9] Gao L, Hwang Y, Cao T. An overview of optimization technologies applied in combined cooling, heating and power systems. Renewable and Sustainable Energy Reviews 2019;114:109344. https://doi.org/10.1016/j.rser.2019.109344.

[10] Liu M, Shi Y, Fang F. Combined cooling, heating and power systems: A survey. Renewable and Sustainable Energy Reviews 2014;35:1-22. https://doi.org/10.1016/j.rser.2014.03.054.

[11] Yang K, Zhu N, Ding Y, Chang C, Wang D, Yuan T. Exergy and exergoeconomic analyses of a combined cooling, heating, and power (CCHP) system based on dual-fuel of biomass and natural gas. Journal of Cleaner Production 2019;206:893-906. https://doi.org/10.1016/j.jclepro.2018.09.251.

[12] Afzali S F, Mahalec V. Novel performance curves to determine optimal operation of CCHP systems. Applied Energy 2018;226:1009-36. https://doi.org/10.1016/j.apenergy.2018.06.024.

[13] Jing R, Zhu X, Zhu Z, Wang W, Meng C, Shah N, Li N, Zhao Y. A multi-objective optimization and multi-criteria evaluation integrated framework for distributed energy system optimal planning. Energy Conversion and Management 2018;166:445-62. https://doi.org/10.1016/j.enconman.2018.04.054.

[14] Cho H, Mago P J, Luck R, Chamra L M. Evaluation of CCHP systems performance based on operational cost, primary energy consumption, and carbon dioxide emission by utilizing an optimal operation scheme. Applied Energy 2009;86(12):2540-9. https://doi.org/10.1016/j.apenergy.2009.04.012.

[15] Yan R, Wang J, Huo S, Zhang J, Tang S, Yang M. Comparative study for four technologies on flexibility improvement and renewable energy accommodation of combined heat and power system. Energy 2023;263:126056. https://doi.org/10.1016/j.energy.2022.126056.

[16] Ju L, Tan Z, Li H, Tan Q, Yu X, Song X. Multi-objective operation optimization and evaluation model for CCHP and renewable energy based hybrid energy system driven by distributed energy resources in China. Energy 2016;111:322-40. https://doi.org/10.1016/j.energy.2016.05.085.

[17] Song X, Liu L, Zhu T, Zhang T, Wu Z. Comparative analysis on operation strategies of CCHP system with cool thermal storage for a data center. Applied Thermal Engineering 2016;108:680-8. https://doi.org/10.1016/j.applthermaleng.2016.07.142.

[18] Wang J, Zhai Z, Jing Y, Zhang C. Particle swarm optimization for redundant building cooling heating and power system. Applied Energy 2010;87(12):3668-79. https://doi.org/10.1016/j.apenergy.2010.06.021.

[19] Mancarella P. Cogeneration systems with electric heat pumps: Energy-shifting properties and equivalent plant modelling. Energy Conversion and Management 2009;50(8):1991-9. https://doi.org/10.1016/j.enconman.2009.04.010.

[20] Zhai X Q, Wang X L, Pei H T, Yang Y, Wang R Z. Experimental investigation and optimization of a ground source heat pump system under different indoor set temperatures. Applied Thermal Engineering 2012;48:105-16.

https://doi.org/10.1016/j.applthermaleng.2012.05.005.

[21] Zeng R, Li H, Liu L, Zhang X, Zhang G. A novel method based on multi-population genetic algorithm for CCHP–GSHP coupling system optimization. Energy Conversion and Management 2015;105:1138-48. https://doi.org/10.1016/j.enconman.2015.08.057.

[22] Zeng R, Zhang X, Deng Y, Li H, Zhang G. An off-design model to optimize CCHP-GSHP system considering carbon tax. Energy Conversion and Management 2019;189:105-17. https://doi.org/10.1016/j.enconman.2019.03.062.

[23] Liu W, Chen G, Yan B, Zhou Z, Du H, Zuo J. Hourly operation strategy of a CCHP system with GSHP and thermal energy storage (TES) under variable loads: A case study. Energy and Buildings 2015;93:143-53. https://doi.org/10.1016/j.enbuild.2015.02.030.

[24] Yuan J, Xiao Z, Zhang C, Gang W. A control strategy for distributed energy system considering the state of thermal energy storage. Sustainable Cities and Society 2020;63:102492. https://doi.org/10.1016/j.scs.2020.102492.

[25] Wang J, Deng H, Qi X. Cost-based site and capacity optimization of multi-energy storage system in the regional integrated energy networks. Energy 2022;261:125240. https://doi.org/10.1016/j.energy.2022.125240.

[26] Yuan J, Cui C, Xiao Z, Zhang C, Gang W. Performance analysis of thermal energy storage in distributed energy system under different load profiles. Energy Conversion and Management 2020;208:112596. https://doi.org/10.1016/j.enconman.2020.112596.

[27] Kang S, Li H, Liu L, Zeng R, Zhang G. Evaluation of a novel coupling system for various load conditions under different operating strategies. Energy Conversion and Management 2016;109:40-50. https://doi.org/10.1016/j.enconman.2015.11.045.

[28] Mago P J, Chamra L M, Ramsay J. Micro-combined cooling, heating and power systems hybrid electric-thermal load following operation. Applied Thermal Engineering 2010;30(8):800-6. https://doi.org/10.1016/j.applthermaleng.2009.12.008.

[29] Ma W, Fang S, Liu G. Hybrid optimization method and seasonal operation strategy for distributed energy system integrating CCHP, photovoltaic and ground source heat pump. Energy 2017;141:1439-55. https://doi.org/10.1016/j.energy.2017.11.081.

[30] Yang G, Zhai X. Optimization and performance analysis of solar hybrid CCHP systems under different operation strategies. Applied Thermal Engineering 2018;133:327-40. https://doi.org/10.1016/j.applthermaleng.2018.01.046.

[31] Kang L, Yang J, An Q, Deng S, Zhao J, Wang H, Li Z. Effects of load following operational strategy on CCHP system with an auxiliary ground source heat pump considering carbon tax and electricity feed in tariff. Applied Energy 2017;194:454-

66. https://doi.org/10.1016/j.apenergy.2016.07.017.

[32] Wang J, Sui J, Jin H. An improved operation strategy of combined cooling heating and power system following electrical load. Energy 2015;85:654-66. https://doi.org/10.1016/j.energy.2015.04.003.

[33] Zheng C Y, Wu J Y, Zhai X Q, Wang R Z. A novel thermal storage strategy for CCHP system based on energy demands and state of storage tank. International Journal of Electrical Power & Energy Systems 2017;85:117-29. https://doi.org/10.1016/j.ijepes.2016.08.008.

[34] Zhou Y, Wang J, Dong F, Qin Y, Ma Z, Ma Y, Li J. Novel flexibility evaluation of hybrid combined cooling, heating and power system with an improved operation strategy. Applied Energy 2021;300:117358. https://doi.org/10.1016/j.apenergy.2021.117358.

[35] Zheng C Y, Wu J Y, Zhai X Q. A novel operation strategy for CCHP systems based on minimum distance. Applied Energy 2014;128:325-35. https://doi.org/10.1016/j.apenergy.2014.04.084.

[36] Feng L, Dai X, Mo J, Ma Y, Shi L. Analysis of energy matching performance between CCHP systems and users based on different operation strategies. Energy Conversion and Management 2019;182:60-71. https://doi.org/doi.org/10.1016/j.enconman.2018.12.006.

[37] Li Y, Tian R, Wei M, Xu F, Zheng S, Song P, Yang B. An improved operation strategy for CCHP system based on high-speed railways station case study. Energy Conversion and Management 2020;216:112936. https://doi.org/10.1016/j.enconman.2020.112936.

[38] Gao Z, Yu J, Zhao A, Hu Q, Yang S. Optimal chiller loading by improved parallel particle swarm optimization algorithm for reducing energy consumption. International Journal of Refrigeration 2022;136:61-70. https://doi.org/10.1016/j.ijrefrig.2022.01.014.

[39] Jia L, Wei S, Liu J. A review of optimization approaches for controlling water-cooled central cooling systems. Building and Environment 2021;203:108100. https://doi.org/10.1016/j.buildenv.2021.108100.

[40] Sun F, Yu J, Zhao A, Zhou M. Optimizing multi-chiller dispatch in HVAC system using equilibrium optimization algorithm. Energy Reports 2021;7:5997-6013. https://doi.org/10.1016/j.egyr.2021.09.012.

[41] Lee K-P, Cheng T-A. A simulation–optimization approach for energy efficiency of chilled water system. Energy and Buildings 2012;54:290-6. https://doi.org/10.1016/j.enbuild.2012.06.028.

[42] Dai Y, Jiang Z, Shen Q, Chen P, Wang S, Jiang Y. A decentralized algorithm for optimal distribution in HVAC systems. Building and Environment 2016;95:21-31. https://doi.org/10.1016/j.buildenv.2015.09.007.

[43] ASHRAE, *2015 ASHRAE Handbook HVAC Applications*. 2015: Atlanta: ASHRAE.

[44] Hope Deepblue Air Conditioning Manufacture Corp. L. *LiBr Chiller*. 2023 [cited 2023; Available from: http://www.slhvac.com/list-12-1.html.

[45] Cold Refrigeration Equipment Corp. L. *Heat pumps*. 2023 [cited 2023; Available from: http://www.coldcn.com/product/index/cid/94.html.

[46] the Solar Energy Laboratory U o W-M a T E S S, LLC, *TRNSYS 18 Documentation Volume 4 Mathematical Reference*. 2017.

[47] De Soto W, Klein S A, Beckman W A. Improvement and validation of a model for photovoltaic array performance. Solar Energy 2006;80(1):78-88. https://doi.org/10.1016/j.solener.2005.06.010.

[48] Zhang Y, Akkurt N, Yuan J, Xiao Z, Wang Q, Gang W. Study on model uncertainty of water source heat pump and impact on decision making. Energy and Buildings 2020;216:109950. https://doi.org/doi.org/10.1016/j.enbuild.2020.109950.

[49] China M o E a W o t P s R o. *Notice on key work related to the reporting and management of enterprise greenhouse gas emissions in 2022*. 2022; Available from: https://www.mee.gov.cn/xxgk2018/xxgk/xxgk06/202203/t20220315_971468.html.